Cellular Microbiology (2015) **17**(3), 355–368
doi:10.1111/cmi.12370
First published online 25 November 2014

Distinct properties of the egress-related osmiophilic bodies in male and female gametocytes of the rodent malaria parasite *Plasmodium berghei*

Anna Olivieri,[1†] Lucia Bertuccini,[2†] Elena Deligianni,[3] Blandine Franke-Fayard,[4] Chiara Currà,[1] Inga Siden-Kiamos,[3] Eric Hanssen,[5] Felicia Grasso,[1] Fabiana Superti,[2] Tomasino Pace,[1] Federica Fratini,[1] Chris J. Janse[4] and Marta Ponzi[1*]

[1]*Istituto Superiore di Sanità, Dipartimento di Malattie Infettive, Parassitarie ed Immunomediate, Rome, Italy.*
[2]*Istituto Superiore di Sanità, Dipartimento di Tecnologia e Salute, Rome, Italy.*
[3]*Institute of Molecular Biology and Biotechnology, FORTH, Heraklion, Greece.*
[4]*Leiden Malaria Research Group, Department of Parasitology, Centre for Infectious Diseases, Leids Universitair Medisch Centrum (LUMC), Leiden, The Netherlands.*
[5]*Bio21 Molecular Science and Biotechnology Institute, Electron Microscopy Unit and Department of Biochemistry and Molecular Biology, University of Melbourne, Melbourne, Australia.*

Summary

Gametogenesis is the earliest event after uptake of malaria parasites by the mosquito vector, with a decisive impact on colonization of the mosquito midgut. This process is triggered by a drop in temperature and contact with mosquito molecules. In a few minutes, male and female gametocytes escape from the host erythrocyte by rupturing the parasitophorous vacuole and the erythrocyte membranes. Electron-dense, oval-shaped organelles, the osmiophilic bodies (OB), have been implicated in the egress of female gametocytes. By comparative electron microscopy and electron tomography analyses combined with immunolocalization experiments, we here define the morphological features distinctive of male secretory organelles, hereafter named MOB (male osmiophilic bodies). These organelles appear as club-shaped, electron-dense vesicles, smaller than female OB. We found that a drop in temperature triggers MOB clustering, independently of exposure to other stimuli. MDV1/PEG3, a protein associated with OB in *Plasmodium berghei* females, localizes to both non-clustered and clustered MOB, suggesting that clustering precedes vesicle discharge. A *P. berghei* mutant lacking the OB-resident female-specific protein Pbg377 displays a dramatic reduction in size of the OB, accompanied by a delay in female gamete egress efficiency, while female gamete fertility is not affected. Immunolocalization experiments indicated that MDV1/PEG3 is still recruited to OB-remnant structures.

Introduction

Plasmodium, the agent of malaria disease, causes 207 million new cases and more than half a million deaths annually (WHO World Malaria Report, 2013). During its complex life cycle, malaria parasites alternate between a vertebrate host and a mosquito vector of the genus *Anopheles*. Parasites injected by an infected mosquito undergo an asymptomatic multiplication inside host hepatocytes. Subsequently, thousands of merozoites are released into the circulation, where they invade red blood cells (RBC). With the exception of invasive, short-lived merozoites, liver and blood stages are obligate intracellular parasites. They develop inside a parasitophorous vacuole (PV), the membrane of which (PVM) represents an interface between parasite and host cell cytoplasm (Zuccala and Baum, 2011). Asexual blood stages are responsible for symptoms associated with malaria disease, while circulating non-replicative gamete precursors (gametocytes) mediate transmission. When male and female gametocytes are ingested by a female mosquito during a blood meal, gamete differentiation (gametogenesis) is triggered by a drop in temperature and contact with molecules of the mosquito midgut microenvironment, such as xanthurenic acid (XA; Billker *et al.*, 1998). A signalling cascade is activated, which involves a

Received 14 January, 2014; revised 20 August, 2014; accepted 08 September, 2014. *For correspondence. E-mail marta.ponzi@iss.it; Tel. (+39) 0649902868; Fax (+39) 0649902226.
†Anna Olivieri and Lucia Bertuccini have contributed equally to the work.

rapid rise of cytosolic calcium (Billker *et al*., 2004) and protein kinase G activation (McRobert *et al*., 2008).

Molecular events leading to gamete maturation and egress from host erythrocyte occur over a short time (15–20 min; Sinden, 1983). The female gametocyte escapes from the host erythrocyte by forming a single macrogamete, competent for fertilization. In contrast, prior to male gametocyte egress from the host cell, three rounds of DNA replication take place in these cells, followed by nuclear division. Eight axonemes are assembled, finally resulting in the release of eight flagellated microgametes. With rapid swimming movements, they reach and then fertilize female macrogametes, therewith initiating the mosquito stages (reviewed in Pradel, 2007).

Egress from the host cell is central both for proliferation of asexual stages and transmission to the mosquito vector. Asexual merozoite escape from the host erythrocyte has been investigated in detail in the human malaria parasite *Plasmodium falciparum* (reviewed in Blackman and Carruthers, 2013). An inside-out model of merozoite egress was experimentally confirmed. Parasitophorous vacuolar membrane disruption was found to be preceded by swelling of the PV compartment and shrinkage of the erythrocyte cytoplasm (Glushakova *et al*., 2005; Chandramohanadas *et al*., 2011). Gametocyte activation and egress was investigated both in the human malaria parasite *P. falciparum* and in the rodent *P. berghei*. As in the case of asexual merozoites, activated gametocytes emerge from the host cell by an inside-out process, which involves PVM rupture at multiple sites (Sologub *et al*., 2011; Deligianni *et al*., 2013) followed by disruption of erythrocyte membrane (EM) at a single breakage point (Sologub *et al*., 2011). The essential role of a perforin-like protein (PPLP2) in EM disruption during microgamete egress was shown in *P. berghei* (Deligianni *et al*., 2013).

Growing evidence implicated electron-dense membrane-bound organelles, referred to as osmiophilic bodies (OB) in egress of activated gametocytes. Ultrastructural studies showed that OB migrate to the gametocyte plasma membrane upon activation (Sinden *et al*., 1976; Aikawa *et al*., 1984). OB disappear after discharging their content into the PV, concurrently with PVM disruption (Sologub *et al*., 2011).

Three OB residents, gametocyte-specific molecules, have been implicated in the egress process. The Pfg377 protein (PF3D7_1250100), expressed in female gametocytes of *P. falciparum*, has a role in OB biogenesis (Alano *et al*., 1995; Severini *et al*., 1999). Deletion of the encoding gene causes a dramatic reduction in OB number and a significant decrease in female gametocyte egress efficiency (de Koning-Ward *et al*., 2008). This reduced efficiency in escaping from the RBC resulted in a significant reduction of oocysts and sporozoite number when the mutant parasites were transmitted to *Anopheles stephensi* mosquitoes (de Koning-Ward *et al*., 2008). MDV-1/PEG3 has been characterized both in human and rodent malaria parasites. In *P. falciparum* (PF3D7_1216500), it localizes primarily to gametocyte PVM (Furuya *et al*., 2005; Silvestrini *et al*., 2005; Lanfrancotti *et al*., 2007), while in *P. berghei* (PBANKA_143220), it resides exclusively in female OB and in vesicle-like structures of male gametocytes (Ponzi *et al*., 2009). The GEST protein (PBANKA_131270), characterized only in *P. berghei*, co-localizes with MDV1/PEG3 in both male and female gametocytes (Talman *et al*., 2011). *P. berghei* parasites lacking either MDV1/PEG3 (Lal *et al*., 2009; Ponzi *et al*., 2009) or PbGEST (Talman *et al*., 2011) are defective in gametocyte egress. In these parasites, gametocytes of both genders fully develop inside RBC but remain entrapped within the PVM after activation of the gametogenesis process.

These observations provide strong evidence that secretory organelles are central in both male and female gametocyte egress. By combining ultrastructural, immunolocalization and genetic approaches, we defined morphological features characteristic of male-specific secretory organelles and refer to them as MOB. Comparative electron microscopy and electron tomography revealed significant differences in size and morphology between female OB and MOB. We showed that clustering of MOB is an early event in male gametogenesis induced *in vitro*. It requires a drop in temperature (from 37°C to 21°C) but is not dependent on an increase in pH or the presence of XA as activation factors. While the MDV1/PEG3 is associated with both OB and MOB, we found that the *P. berghei* g377, like the *P. falciparum* orthologue, localizes to female OB. In *P. berghei* mutants lacking Pbg377, female gametocytes develop normally but display a dramatic reduction in size of OB that lack their typical oval-shaped morphology. This structural change is accompanied by a delay in egress efficiency but not in female gamete fertility.

Results

Pbg377 localizes to OB of P. berghei *female gametocytes morphologically distinct from secretory vesicles of males*

To characterize expression and localization of the *P. berghei* g377 (Pbg377; PBANKA_146300), we raised mouse antibodies against the C-terminal portion of the protein. The immune serum specificity was confirmed by western blot analysis on purified wild-type (WT) gametocytes and on mixed blood stages of isogenic *P. berghei* parasites (HPE) that are unable to produce gametocytes (Fig. 1A). Two main protein bands were detected exclusively in the gametocyte preparation,

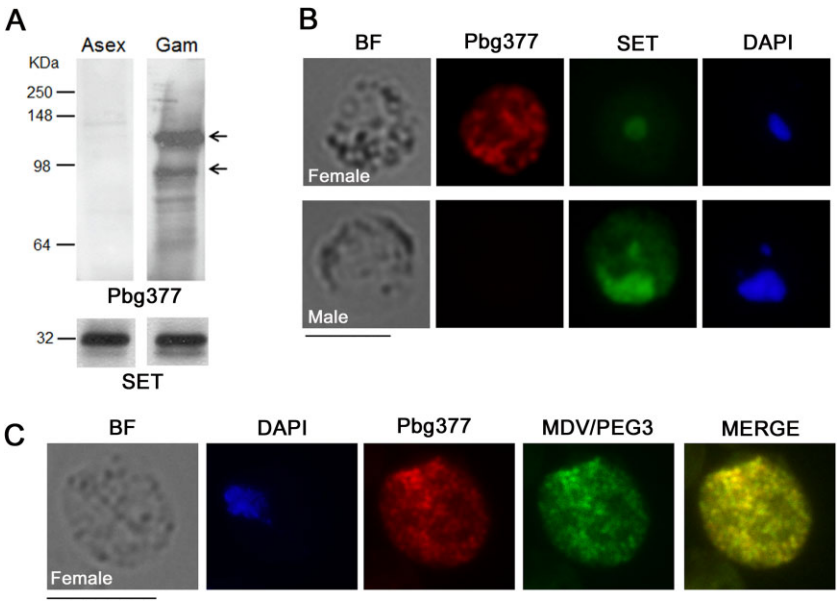

Fig. 1. Female gametocyte-specific expression of Pbg377.
A. Total proteins from mixed blood stages of a non-gametocyte producer *P. berghei* line HPE (Asex) and purified gametocytes (Gam) from WT *P. berghei* parasites were probed with α-Pbg377. Two main protein bands (arrowed) are stained only in the gametocyte sample.
B. WT gametocytes are stained with rabbit antibodies specific for the nuclear protein SET (PBANKA_081990) and mouse antibodies specific for Pbg377. SET is highly abundant in male gametocytes and is used to discriminate between males and females. Representative images show that Pbg377 is present in vesicle-like structures only in female gametocytes.
C. Co-localization experiments, using specific antibodies, show that Pbg377 and MDV1/PEG3 reside in the same vesicular structures of female gametocytes. Bar: 5 μm.

indicating that Pbg377 expression is confined to sexual stages. The presence of multiple bands suggests that Pbg377, as in the case of *P. falciparum* Pfg377, is subjected to post-translational cleavage. The size of the two detected polypeptides does not account for the entire protein (expected size of 309.2 kDa), suggesting the presence of additional fragments not recognized by the antibodies.

In immunofluorescence assay (IFA), Pbg377-specific antibodies stained dot-like structures only in female gametocytes (Fig. 1B). We used antibodies against the nuclear protein SET, which strongly labels the nucleus of male gametocytes (Pace *et al*., 2006), to distinguish between males and females. Double IFA using α-Pbg377 and α-MDV1/PEG3 antibodies showed that these proteins localize to the same vesicular structures (Fig. 1C) in female gametocytes.

Immune electron microscopy (IEM), revealed that both Pbg377 and MDV1/PEG3 reside in the characteristic oval-shaped OB of female gametocytes, while only MDV1/PEG3 was detected in OB-like, electron-dense organelles of male gametocytes (Fig. 2). In transmission electron microscopy (TEM), these appear as elongated, club-shaped structures, smaller than female OB (Fig. 2). Here we define these OB-like organelles 'male osmiophilic bodies' (MOB).

Electron tomography of gametocytes, followed by three-dimensional reconstruction, was employed to compare the size and morphology of OB and MOB. As shown in Fig. 3, the two organelles differ significantly both in morphology and size. Male osmiophilic bodies were found to be more slender than OB, and their volume was only ~1/3 of that of OB.

MOB cluster after activation of male gametocytes

Discharge of the OB content into the PV is believed to be essential for gametocyte egress from the infected RBC. In activated female gametocytes, OB accumulate at the gametocyte plasma membrane in multiple foci, which may be associated with PVM rupture sites (Wirth and Pradel, 2012). Conversely, in activated male gametocytes, MOB seem to coalesce in only a few focal points (Lal *et al*., 2009). To achieve a better understanding of these male-specific organelles, we followed MOB behaviour after gametocyte activation and simultaneously monitored OB for comparison. Gametocytes were activated by a drop in temperature (from 37°C to 21°C) and an increase in pH (from 7.2 to 8.2). After activation, gametocytes were collected at different time points and stained with α-MDV1/PEG3. As shown in Fig. 4A, within the first minute, female OB move to the cell periphery. In contrast, MOB appear to coalesce in a few spots, which display a bright fluorescence (Fig. 4B). Interestingly, we observed that a temperature drop was sufficient to trigger MOB clustering (Fig. 4C and Supporting Information Fig. S1), while discharge of their content, monitored by IFA, occurred within 5–8 min only when the pH was increased (Supporting Information Fig. S2). Parasitophorous vacuolar membrane disruption was verified in parallel by TEM (not shown). It appears that MOB are routed to the parasite plasma membrane as clusters of separated vesicles (Supporting Information Fig. S2). This indicates that the peculiar coalescence of MOB in a few foci is not accompanied by membrane fusion events leading to larger organelles. IEM images confirmed that these clusters are stained by α-MDV1/PEG3 (Fig. 4D).

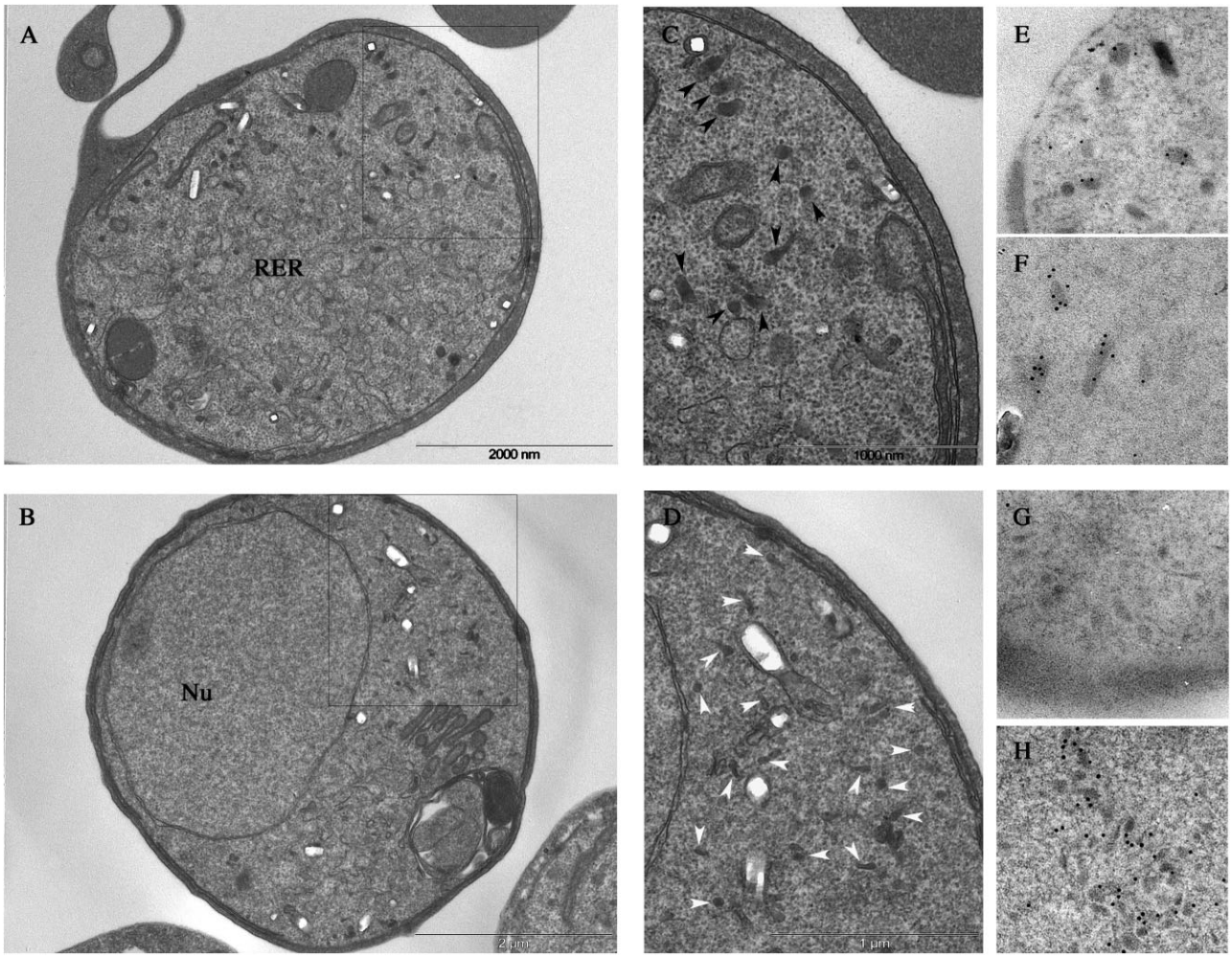

Fig. 2. Ultrastructural analysis and immunogold localization of OB and MOB in *P. berghei* gametocytes.
A. Female gametocytes are characterized by oval shaped OB of more than 100 nm in length (black arrowheads in enlarged section C). Immunogold labelling using antibodies-specific forPbg377 and MDV1/PEG3 detects both Pbg377 (E) and MDV1/PEG3 (F) in female-specific OB.
B. Male gametocytes are characterized by elongated, club-shaped MOB less than 100 nm in length (white arrowheads in enlarged section D). MOB are stained by MDV1/PEG3 (H), but not by Pbg377 (G) specific antibodies.

Conversely, early after activation, OB migrate to the cell periphery as separate vesicles (Supporting Information Fig. S2). We never observed OB clustering in activated *P. berghei* females.

In order to determine whether mobilization of Ca^{2+} stores in gametocytes is implicated in OB and MOB dynamics, we treated mature gametocytes with the Ca^{2+} chelator 1,2-Bis(2-aminophenoxy)ethane-N,N,N′,N′-tetraacetic acid tetrakis(acetoxymethyl ester) (BAPTA-AM). It has been shown that treatment of gametocytes with BAPTA-AM blocks Ca^{2+} mobilization in the cytosol, thereby inhibiting early events associated with gametogenesis (Billker *et al.*, 2004). Gametocytes were incubated with 100 µM BAPTA-AM and then activated. After 20 min of incubation at 37°C, chelator treatment resulted in a block of exflagellation (data not shown). We then stained OB and MOB in activated gametocytes with α-Pbg377 or α-MDV1/PEG3 antibodies. This analysis revealed that the block of Ca^{2+} release inhibits the dynamics of both OB and MOB, i.e. the migration to the cell periphery or clustering (Supporting Information Fig. S3). Interestingly, this treatment also affects recruitment of the protein SET into the nucleus.

OB number and morphology is affected in female gametocytes lacking Pbg377

In order to define the role of the OB-resident protein Pbg377 in *P. berghei* gametocytes, we used standard genetic modification technologies to delete the *Pbg377* gene. In two independent transfection experiments, we successfully generated and selected gene deletion

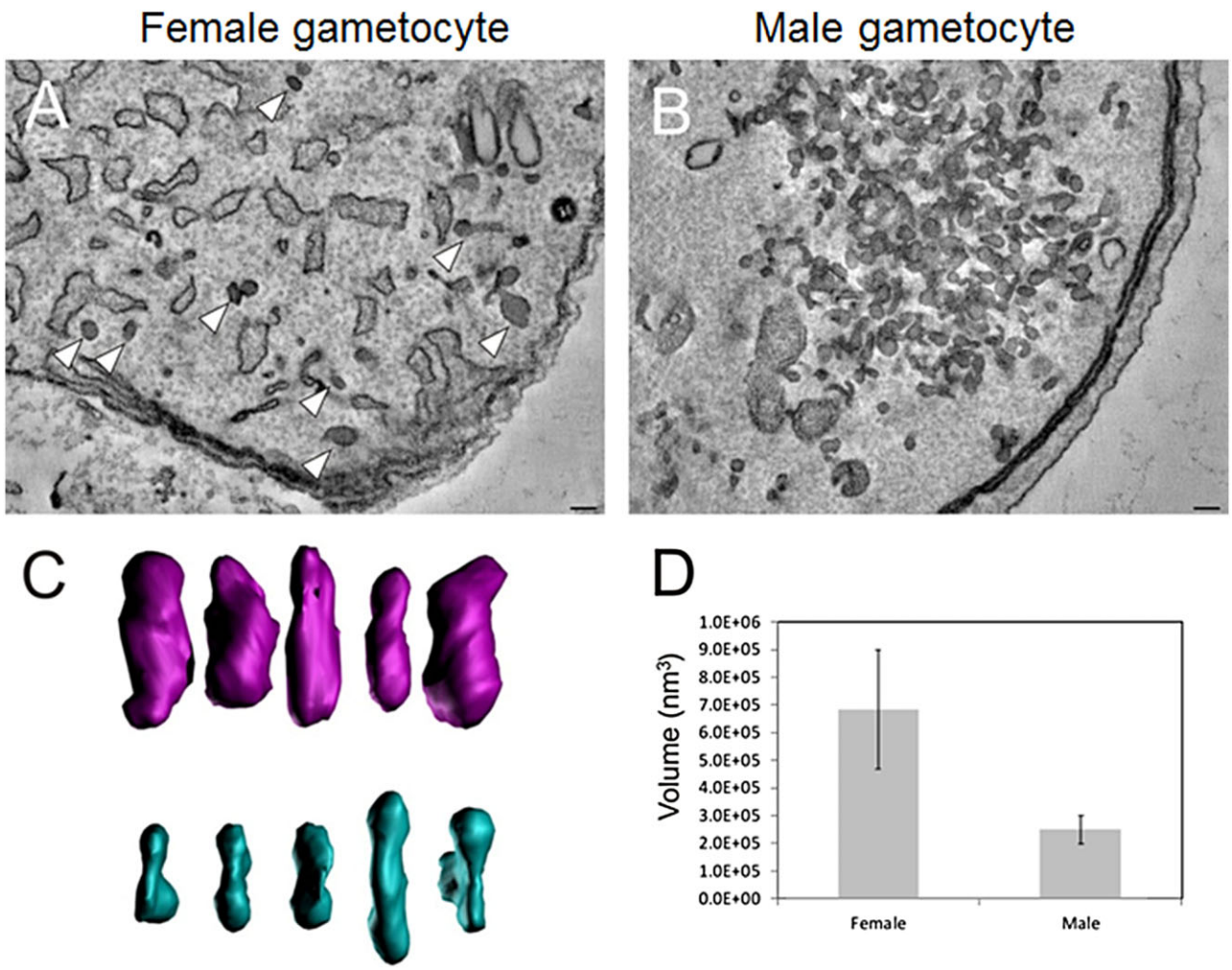

Fig. 3. Electron tomography of WT gametocytes. Virtual sections (5 nm) showing:
A. Female gametocyte OB (arrowhead).
B. Male gametocyte club-shaped MOB.
C. Rendered OB (top row) and MOB (bottom row).
D. Volume of OB and MOB calculated from the tomograms. Scale bars, 100 nm.

mutants (Supporting Information Fig. S4A). The cloned lines *ΔPbg377-a* (600cl1) and *ΔPbg377-b* (622cl1) were used for genotyping. Genotype and Southern analyses of digested DNA and/or of chromosomes separated by pulse field gel electrophoresis, confirmed correct deletion of the *Pbg377* gene (Supporting Information Fig. S4B). Northern analysis showed the absence of *Pbg377* transcripts (Supporting Information Fig. S4C). The lack of the encoded protein was demonstrated by IFA and western blot analysis on mature gametocytes of the mutant lines (Fig. 5).

TEM analysis of *ΔPbg377* female gametocytes did not detect typical OB but only tiny osmiophilic vesicles, which were reduced in size compared with OB of WT females (Fig. 6). The altered morphology of OB in mutant parasites was confirmed by determining minimum and maximum size values of more than a hundred OB sections present in TEM micrographs of WT and *ΔPbg377* gametocytes (Supporting Information Fig. S5). These observations indicate that Pbg377 may have a structural role in defining the shape of female OB. Absence of this protein does not result in a near complete lack of OB, as described for *P. falciparum* mutant lacking Pfg377, but instead results in a dramatic change in OB morphology. Notably, in *ΔMDV/PEG3*, a mutant lacking expression of MDV1/PEG3 (Ponzi *et al.*, 2009), OB size is comparable to that of WT female gametocytes (Supporting Information Fig. S6A).

MDV1/PEG3 localizes to OB-like structures in ΔPbg377

We asked whether subcellular localization of MDV/PEG3, detected both in OB and MOB of WT gametocytes, is

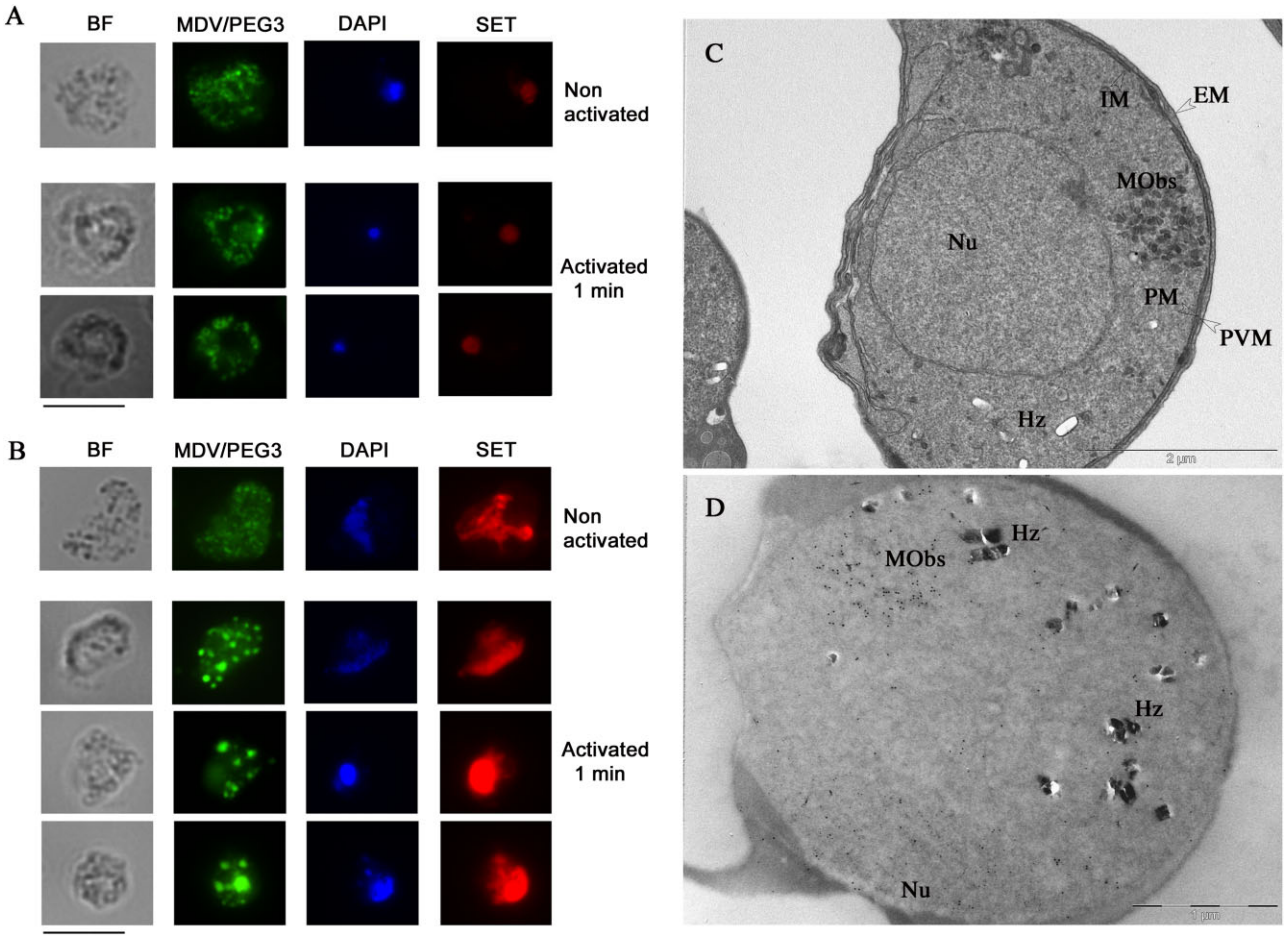

Fig. 4. MOB coalesce early after male gametocyte activation. Gametocytes 1 min after activation were fixed and stained with MDV1/PEG3-specific antibodies. Males and females were distinguished using antibodies against the nuclear protein SET, highly abundant in male gametocytes. OB localize to the cell periphery in the majority of activated females (A) while MOB progressively coalesce in few foci (B). TEM micrograph of a mature male gametocyte subjected to a drop in temperature shows that clustered MOB do not fuse as they maintain distinct membranes. The inner membrane complex (IM), at the periphery of male gametocyte, is not uniformly distributed and presents frequent discontinuities (C). MDV1/PEG3-specific antibodies (10 nm gold particles) are associated with MOB clusters. The large, eccentric nucleus of the male gametocyte is stained by SET-specific antibodies (5 nm gold particles) (D). Nu, nucleus; EM, erythrocyte membrane; PM, parasite membrane; PVM, parasitophorous vacuole membrane; Hz, hemozoin pigment. Scale bar, 5 µm.

affected in *ΔPbg377* gametocytes. In immunolocalization experiments, MDV1/PEG3-specific antibodies mark dot-like structures of both female and male gametocytes of *ΔPbg377* (Supporting Information Fig. S6B). This suggests that secretory organelles are still present in both genders of the *ΔPbg377* mutant parasites. We next followed the dynamics of MDV/PEG3-positive OB and MOB in *ΔPbg377* gametocytes. One minute after activation, OB stained by MDV/PEG3 antibodies relocate to the gametocyte periphery, while MOB tend to form clusters (Supporting Information Fig. S7). These observations support the notion that *ΔPbg377* female gametocytes still contain OB-like structures, which are able to respond to drop in temperature and pH increase similarly to OB of WT female gametocytes.

We were unable to decorate OB-like structures in *ΔPbg377* females by IEM using MDV1/PEG3-specific antibodies, whereas these antibodies readily detected OB of the WT gametocytes in IEM and both WT and *ΔPbg377* OB in IFA. This lack of staining of *ΔPbg377* OB in IEM might be due to the small size of OB in *ΔPbg377* females, which prevents efficient labelling.

Female gametocytes lacking Pbg377 are fertile although egress is delayed

As expected, *ΔPbg377* parasites showed WT asexual multiplication rates *in vivo* (Supporting Information Table S1). Production of gametocytes was slightly reduced in clone *ΔPbg377-b* (622cl1) compared with WT,

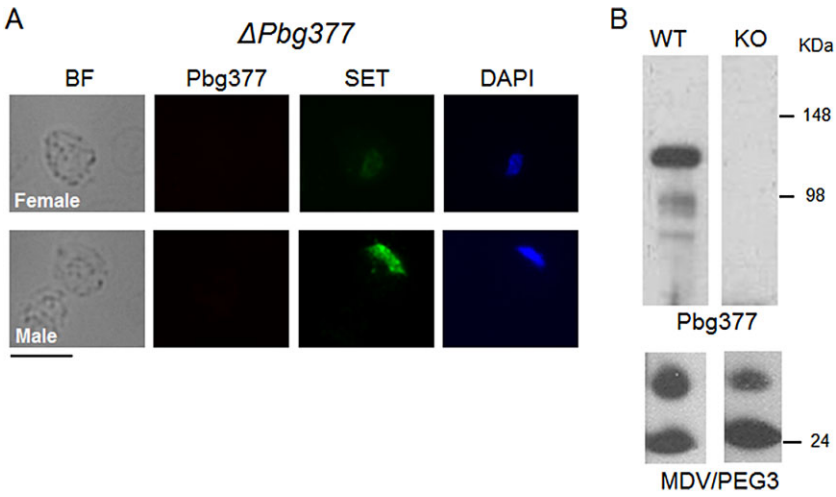

Fig. 5. Characterization of *ΔPbg377* parasites.
A. Male and female gametocytes of *ΔPbg377* mutant were subjected to double IFA using mouse α-Pbg377 and rabbit α-SET antibodies. Representative images show that Pbg377 is absent in *ΔPbg377* sexual stages.
B. Mature gametocytes purified from WT and *ΔPbg377* mutant (KO) were probed with α-Pbg377 immune serum and successively with α-MDV1/PEG3 as a loading control.
Scale bar, 5 μm.

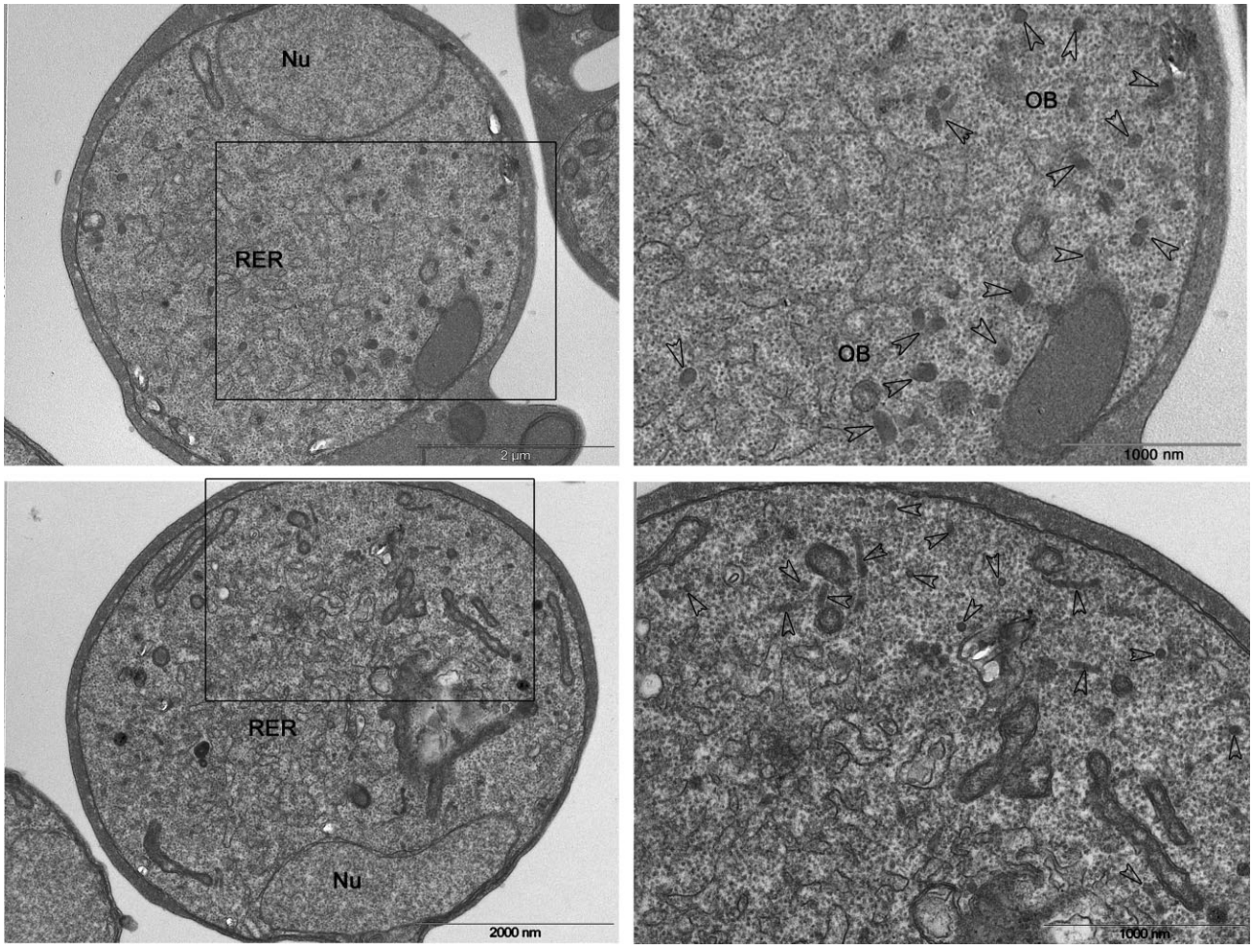

Fig. 6. Ultrastructural analysis of *ΔPbg377* and WT gametocytes. Female gametocytes of *ΔPbg377* (bottom panels) are characterized by OB smaller in size than WT female gametocyte OB (top panels). OB are arrowed in enlarged sections. RER, rough endoplasmic reticulum; Nu, nucleus.

while the other clone examined was similar to WT (Supporting Information Table S1). Standard *in vitro* ookinete production assays were performed to determine the percentage of female gametes that transform into ookinetes. Ookinete production of *ΔPbg377* was similar to WT parasites (Supporting Information Table S1). Analysis of oocyst and sporozoites production in *Anopheles stephensi* confirmed the normal fertility of *ΔPbg377* (Table S1).

P. falciparum female gametocytes lacking Pfg377 are delayed in egress from the host erythrocyte. We therefore analysed in detail egress of *P. berghei* males and females. Gametocytes of the WT and *ΔPbg377* parasites were collected from infected mice and activated by dilution in RPMI supplemented with XA. 15 and 20 min after activation, parasites were fixed and immunolabelled with TER-119, an antibody against a RBC surface protein. To distinguish between male and female gametocytes, we made use of the SET antibody and DNA staining. 15 min post-activation a reduction of approximately 60% in female egress was observed in mutant parasites compared with the WT, while males emerged normally, as expected (Fig. 7). At 20 min, egress of mutant female gametocytes was comparable to the WT. These observations indicate that in the absence of normal OB, female gametocytes are able to egress from the host erythrocyte, although less efficiently than the WT.

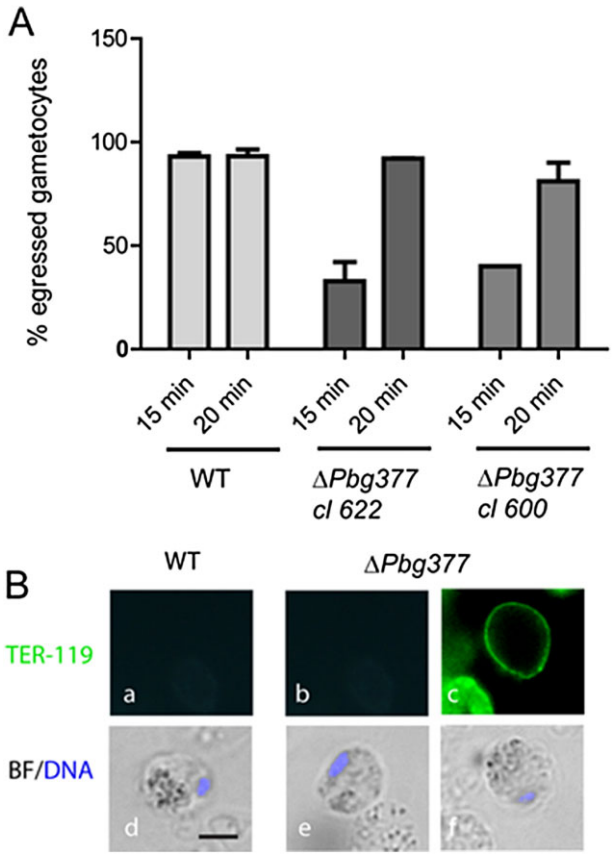

Fig. 7. Delay of egress of *ΔPbg377* female gametocytes.
A. Gametocytes were fixed at 15 and 20 min after activation. α-SET immunolabelling and staining of DNA was used to distinguish between male and female parasites. Egress was assessed by the presence or absence of anti-TER-119 signal surrounding the cell. WT, light grey bars. *ΔPbg377 cl 622cl1* and *clone 600cl1*, dark grey bars. The data represent pooled results from two independent experiments of each *ΔPbg377* clone and four WT experiments. At least 50 cells were counted in each sample. $P < 0.01$, Student's *t*-test comparing WT pairwise with each *ΔPbg377* clone.
B. Representative images of female gametocytes labelled with α-TER-119. a, d: Egressed WT gametocyte. b, e: Egressed *ΔPbg377* gametocyte. c, f: *ΔPbg377* gametocyte still enclosed in the host cell membrane. Scale bar, 5 μm.

Discussion

Escape from the host cell is essential for survival of intracellular parasites. In *Plasmodium*, this key process is tightly regulated and leads to the eventual rupture of PVM and host cell membrane with an inside-out mechanism (reviewed in Wirth and Pradel, 2012; Blackman and Carruthers, 2013). In sexual stages of both *P. falciparum* and *P. berghei*, PVM ruptures at multiple sites soon after activation, concomitant with the discharge of OB, specialized electron-dense secretory organelles, specific for female gametocytes (Sologub *et al.*, 2011; Deligianni *et al.*, 2013; Andreadaki *et al.*, unpublished).

Functional studies on these key organelles are difficult because of the limited number of OB-associated molecules characterized so far. In *P. berghei*, MDV1/PEG3 (Ponzi *et al.*, 2009) and GEST (Talman *et al.*, 2011) were detected in vesicle-like structures of both genders. IEM or co-immunolocalization studies confirmed that both MDV1/PEG3 (Ponzi *et al.*, 2009) and PbGEST (Talman *et al.*, 2011) mark female gametocyte OB. The female-specific Pfg377 is the only protein associated to OB of *P. falciparum* gametocytes (Alano *et al.*, 1995). The lack of this molecule causes a significant delay in female gamete egress (de Koning-Ward *et al.*, 2008), likely because of a dramatic reduction in OB number.

We show here that the *P. berghei* orthologue, Pbg377, is a female-specific protein and localizes to OB. Co-immunolocalization experiments indicated that Pbg377 and MDV1/PEG3 mark the same vesicular structures in female gametocytes, suggesting that OB are homogeneous in protein content.

In parasites deficient for Pbg377 (*ΔPbg377*), we observed a delay in female gametocyte egress, while males escape normally from RBC. The percentage of gametes that transform into ookinetes *in vitro* was not

affected, indicating no defect in fertility of macrogametes. This was also confirmed *in vivo* through the analysis of oocysts and sporozoites produced in *Anopheles stephensi* mosquitoes. Taken together, these observations suggest that, although a delay in egress is detectable, fertility of the females is not compromised.

TEM analysis of female gametocytes lacking Pbg377 showed electron-dense, OB-like structures that were significantly reduced in size, compared with OB of WT female gametocytes, In contrast, OB morphology is not affected in *ΔMDV/*PEG3, a mutant lacking expression of MDV1/PEG3 (Ponzi *et al*., 2009). These observations strongly support a structural role of Pbg377 in the biogenesis of these organelles. However, lack of Pbg377 does not prevent recruitment of egress-related proteins into OB-remnant structures. We, in fact, detected MDV1/PEG3 in *ΔPbg377* female gametocytes. MDV1/PEG3-containing vesicular structures respond to a drop in temperature and increase of pH, similarly to OB of WT gametocytes, and may support, although less efficiently, female gametocyte egress.

In contrast to Pbg377, the OB-resident proteins MDV1/PEG3 (Ponzi *et al*., 2009) and GEST (Talman *et al*., 2011) have a clear role in egress of both male and female *P. berghei* gametocytes. In the absence of these proteins, both sexes are severely affected in emergence from the RBC, although no alteration in OB shape or in the ability to discharge their content was observed in *ΔMDV/*PEG3 (this study and Ponzi *et al*., 2009). Recruitment of egress-related proteins into OB and MOB strongly supports a key role of these organelles in gametocyte escape from the host RBC. Moreover, the active involvement of proteins in the egress process indicates that mechanical forces caused by formation of the highly motile male gametes are not sufficient to rupture the PVM/EM membranes in WT parasites. Consistent with these observations is the fact that *P. berghei* parasites lacking a member of plant-like calcium-dependent protein kinases, CDPK4 are still capable to egress from the host cell, despite a severe defect in axoneme formation and lack of exflagellation (Billker *et al*., 2004).

Immune electron microscopy studies detected MDV1/PEG3 in both OB and MOB, while electron tomography revealed distinctive morphological features of these gender-specific electron-dense vesicles. Female OB are oval-shaped and their volume is approximately three times greater than the one of club-shaped MOB.

In non-activated gametocytes, both kinds of vesicles are dispersed throughout the cytoplasm. In activated females, OB are uniformly distributed underneath parasite surface before fusing to the plasma membrane. In activated males, MOB progressively coalesce in few focal points as previously observed (Lal *et al*., 2009). Ultrastructural analysis revealed that MOB become organized in large clusters that, in some cases, come into contact with the parasite membrane. MOB clustering occurs in response to a drop in temperature, but increase of pH or addition of XA is required for efficient vesicle discharge. Under optimal conditions, MDV1/PEG3-specific fluorescence is greatly reduced 5–8 min after activation, suggesting that the majority of MOB released their content over this time.

It is conceivable that release of MOB content into PV and the subsequent PVM disruption occurs in one or few delivery sites and not at multiple points as in the case of females (Sologub *et al*., 2011). Egress of motile males might be similar to egress of asexual merozoites from the host RBC. Breakdown of the host cell membrane by merozoites initiates, in fact, with the formation of a single pore followed by curling of the membrane and a physical ejection of merozoites in the blood (Abkarian *et al*., 2011).

The peculiar spatial organization of secretory vesicles, observed only in activated males, likely reflects a specific mechanism of vesicle discharge. The best described case of vesicle clustering has been reported for small synaptic vesicles (SVs), which fuse with the plasma membrane and release neurotransmitters in response to a wide variety of stimuli (reviewed in Shupliakov *et al*., 2011). Electron tomographic studies showed that SVs are held together by filaments and elongated proteins. The nature of these inter-vesicular tethers has not been completely elucidated. The dynamics of SV clustering is regulated by the phosphorylation state, while destabilization of the intra-vesicular matrix and membrane fusion events are likely triggered by Ca^{2+} influx and de-phosphorylation.

Local increase of Ca^{2+} concentration and activation of calcium-dependent protein kinases are required for egress of Apicomplexan parasites *Toxoplasma gondii* and *P. falciparum* (reviewed in Blackman and Carruthers, 2013). It has been shown that treatment of gametocytes with the Ca^{2+} chelator BAPTA-AM blocks Ca^{2+} mobilization in the gametocyte cytosol and thereby inhibiting early events associated with gametogenesis (Billker *et al*., 2004). We observed that both OB repositioning to the female gametocyte periphery and MOB clustering are affected in gametocytes treated with BAPTA-AM. These observations indicate that OB dynamics is dependent on Ca^{2+} release.

Evidence presented in this study indicates that molecular events leading to gametocyte egress differ between female and male gametocytes. A further dissection of this process, essential for fertilization and development within the mosquito, may provide knowledge for designing strategies that can effectively block transmission.

Experimental procedures

Experimental animals and P. berghei *ANKA reference lines*

Female Swiss OF1 mice (6–8 weeks) from Charles River were used. All animal experiments performed at the LUMC were approved by the Animal Experiments Committee of the Leiden University Medical Center (DEC 07171; DEC 10099). The Dutch Experiments on Animal Act is established under European guidelines (EU directive no. 86/609/EEC regarding the Protection of Animals used for Experimental and Other Scientific Purposes).

P. berghei ANKA parasite lines used in this study were the WT reference line cl15cy1 (Janse *et al*., 2006) and the non-gametocyte producer line HPE.

Generation and genotyping of mutants lacking Pbg377 (ΔPbg377)

To disrupt the *Pbg377* gene (PBANKA_146300), the standard plasmid pL0001 (MRA-770, http://www.mr4.org) was used, which contains the pyrimethamine resistant *T gondii* (*Tg*) dihydrofolate reductase-thymidylate synthase (*dhfr/ts*) as a selectable marker (SM) under the control of the *P. berghei dhfr/ts* promoter. Targeting sequences for homologous recombination were polymerase chain reaction (PCR) amplified from *P. berghei* ANKA (cl15cy1) genomic DNA using primers specific for the 5′ or 3′ end of each gene: 2307/2308 (5′-CGGGGTACCcaacaagcaatatgtgcagac; 5'CCCAAGCTTctagtttatctggtatataactagg) and 2309/2310 (5′-CCGGAATTCgcacccccagaatcaaacatag; 5′-CGCGGATCCggtgct gtagtatcgtttaatg). The PCR-amplified target sequences were cloned either upstream or downstream of the SM to allow for integration of the construct into the targeting regions by double crossover homologous recombination. The final DNA construct was linearized with KpnI/BamHI before transfection. Transfection and selection of transformed parasites was performed using standard genetic modification technologies for *P. berghei* (Janse *et al*., 2006) using *P. berghei* ANKA (cl15cy1) as the parent parasite line. Cloned parasite lines were obtained from two independent transfections (exp. 600 and 622) by the method of limiting dilution. Correct integration of DNA constructs and disruption of genes was verified by Southern analyses of digested DNA or of PFGE pulsed-field-gradient electrophoresis (PFG)-separated chromosomes (Janse *et al*., 2006). PFG-separated chromosomes were hybridized with the 3'UTR of *P. berghei dhfr/ts* gene recognizing the endogeneous *dhfr/ts* locus on chromosome 7 and the integrated locus on chromosome 14. Digested DNA (BglII) was hybridized with a probe recognizing the *Tgdhfr/ts* SM. The loss of *Pbg377* transcripts in the gene-deletion mutants was verified by standard Northern blot analyses. Total RNA was isolated from mixed blood stages/purified gametocytes of *P. berghei* ANKA (gametocyte producer line cl15cy1 or the non-gametocyte producer line 2.33) and cloned lines of gene-deletion mutant (600cl1: Δ*Pb377-a*; 622cl1: Δ*Pb377-b*). Northern blots were hybridized with a PCR probe specific for 5'utr of *Pbg377* amplified from *P. berghei* ANKA genomic DNA using primers 2307/2308 (see above). As a loading control, Northern blots were hybridized with the oligonucleotide probe L644R that recognizes the large subunit ribosomal RNA (van Spaendonk *et al*., 2001) or with a Pbs25 gene-specific probe (Braks *et al*., 2008).

Phenotype analysis of ΔPbG377

In vivo *multiplication rate of asexual blood stages.* The multiplication rate of asexual blood stages in mice is determined during the cloning procedure of each gene-deletion mutant (Spaccapelo *et al*., 2010) and is calculated as follows: the percentage of infected erythrocytes in Swiss OF1 mice injected with a single parasite is quantified at days 8 to 11 on Giemsa-stained blood films. The mean asexual multiplication rate per 24 h is then calculated assuming a total of 1.2×10^{10} erythrocytes per mouse (2 mL of blood). The percentage of infected erythrocytes in mice infected with reference lines of the *P. berghei* ANKA strain consistently ranges between 0.5% and 2% at day 8 after infection, resulting in a mean multiplication rate of 10 per 24 h (Janse *et al*., 2003; Spaccapelo *et al*., 2010).

Gametocyte and ookinete production. Gametocyte production is defined as the percentage of ring forms developing into mature gametocytes during synchronized infections (Janse and Waters, 1995). Ookinete production was determined in standard *in vitro* fertilization and ookinete maturation assays and is defined as the percentage of female gametes that develop into mature ookinetes under standardized *in vitro* culture conditions (van Dijk *et al*., 2001). Female gamete and mature ookinete numbers were determined in Giemsa-stained blood smears made 16–18 h post-activation.

Egress. Infected mice with a parasitemia between 5 and 10 % were treated with sulfadiazine for ~ 36 h as described previously (Deligianni *et al*., 2011). The presence of gametocytes, and the minimum contamination of asexual stages, which presence would confound the analysis, was determined in Giemsa-stained blood smears. Blood samples were removed and diluted in RPMI pH 8.0 supplemented with 50 μM XA and kept at 19°C to activate gametogenesis. At 15 and 20 min, samples were removed and fixed by addition of 4% paraformaldehyde in phosphate buffered saline (PBS) for 30 min, and then permeabilized with 0.5% Triton X-100. Samples were then labelled with the α-SET antibody and the 13.1 antibody recognizing the P28 protein found on the surface of female gametes, followed by incubation with secondary antibodies conjugated to Alexa 488 and 555 respectively. The conjugated antibody directed against the TER-119 protein of the mouse erytrocyte was then added, followed by staining of the DNA with Hoechst 33342. Samples were mounted in Vectashield and scored using an Axioscope microscope. Attempts to use the 13.1 antibody recognizing the surface protein P28 on female gametes was unsuccessful for samples activated for 15, although a clear signal was seen in the 20 min samples and onwards (data not shown).

Oocyst and sporozoite production in Anopheles stephensi mosquitoes. For mosquito transmission experiments, female *A. stephensi* mosquitoes were fed on mice infected with WT parasites or mutants. Oocyst development, oocyst production and sporozoite production was monitored in infected mosquitoes as described in (Sinden, 1997). Oocyst and sporozoite numbers were counted in infected mosquitoes at 11–14 days and 19–22 days after infection respectively. Salivary gland sporozoites were isolated and counted as described (Annoura *et al*., 2012).

Sporozoite infectivity. To determine *in vivo* infectivity of sporozoites, Swiss OF1 mice were infected with 1×10^4 salivary gland sporozoites by intravenous injection, as previously described (Sinden, 1997). Blood stage infections were monitored by analysis of Giemsa-stained thin smears of tail blood collected on days 4–8 after inoculation of sporozoites. The prepatent period (measured in days post-sporozoite infection) is defined as the day when a blood stage infection with a parasitemia of 0.5–2% is observed.

TEM

Nycodenz-purified gametocytes were fixed in 2% glutaraldehyde, 2% paraformaldehyde, 2 mM $CaCl_2$ in 0.1 M sodium cacodylate buffer, pH 7.4, overnight at 4°C, and processed according to (Perry and Gilbert, 1979). Parasites were washed in cacodylate buffer and post-fixed with 1% OsO4 in 0.1 M sodium cacodylate buffer for 1 h at RT, treated with 1% tannic acid in 0.05 M cacodylate buffer for 30 min and rinsed in 1% sodium sulphate in 0.05 M cacodylate buffer for 10 min. Post-fixed specimens were washed, dehydrated through a graded series of ethanol solutions (30–100% ethanol) and embedded in Agar 100 (Agar Scientific Ltd, UK). Ultrathin sections, obtained by an UC6 ultramicrotome (Leica), were stained with uranyl acetate and Reynolds' lead citrate and examined by an EM208 Philips electron microscope.

Immunoelectron microscopy

Nycodenz-purified gametocytes were processed for immunoelectron microscopy according to published protocols (Newman, 1989). Briefly, samples were fixed overnight at 4°C with 4% paraformaldehyde/0.1% glutaraldehyde in 0.1 M sodium cacodylate buffer. Next, the suspension was gently washed in sodium cacodylate buffer, dehydrated in ethanol serial dilutions and embedded in LR White, medium-grade acrylic resin (London Resin Company, UK). The samples were polymerized in a 50°C oven for 72 h. Ultrathin sections, collected on gold grids, were sunk in 100% ethanol for 3 min, immersed in Tris buffer 0.05 M (pH 10.0) in PCR tubes, then kept at 99°C for 30 min using a constant temperature box (Saito *et al*., 2003).

For immunostaining, the grids were floated on drops of PBS containing 0.1 M glycine for 10 min, washed with PBS, blocked with 5% normal goat serum/1% BSA in PBS for 30 min. For immunogold-labelling of Pbg377 and MDV1/PEG3, each grid was incubated overnight at 4°C, respectively, on a drop of mouse polyclonal anti-377 serum (1:100) and of mouse polyclonal anti-MDV/PEG3 serum (1:100) in PBS/0.1% BSA/0.05% TWEEN 20 buffer. Grids were then rinsed and incubated for 1h with 10 nm gold-conjugated goat anti-mouse IgG (SIGMA) (1:50), rinsed again in buffer followed by distilled water and finally air-dried.

The ultrathin sections were stained successively with uranyl acetate 2% in H_2O (20 min) and Reynolds' lead citrate solution (3 min), and observed with an EM208 Philips transmission electron microscope. As controls, sections were stained without any heating, without the primary antibody and with the diluted gold anti-mouse IgG, or with the diluted mouse pre-immune serum in place of the primary antibody.

Electron tomography

Purified gametocytes, prepared as previously described (Deligianni *et al*., 2011), were treated for the Reduced osmium fixation (ROTO) technique according to (Hanssen *et al*., 2013). Cells were then embedded in epoxy resin, sectioned to 300 nm and observed on a FEI Tecnai F30 Transmission Electron Micoscope (Bio21 Institute, Electron Microscopy Facility) at 300 kV. Tomograms were collected between −70 and 70 degrees using SerialEM (Mastronarde, 2005) on an Ultrascan 1000 (Gatan, Pleasanton, CA, USA). Tomograms were reconstructed and segmented using the IMOD package (Kremer *et al*., 1996). For tomographic reconstruction, see also Mastronarde (1997).

Antibodies

A Pbg377 fragment amplified using the primers gaccggatccga acatttagaaccatttattcct and gaccgcggccgcttcttgatttcctgatttatc was cloned in the BamHI-NotI sites of the pGEX-6P-1 vector. Pbg377 fragment was expressed and used to produce specific antibodies in BALB/c mice by intraperitoneal injection with 50 μg recombinant protein (first injection in Freund's complete adjuvant; two further injections performed at 2-week intervals in Freund's incomplete adjuvant). Mice were bled 1 week after the third immunization.

Working dilutions of antibodies used in this study were α-Pb377 mouse polyclonal, 1:300 in IFA, 1:2000 in western blot; α-MDV/PEG3 mouse polyclonal, 1:400 in IFA, 1:2000 in western blot; α-SET rabbit polyclonal (Pace *et al*., 2006) 1:200 in IFA, 1:5000 in western blot; Alexa Fluor 488 α-mouse TER-119 (BioLegend) 1:400 in IFA.

Indirect IFA

Immunofluorescence assay was performed at room temperature as follows: blood smears were fixed on glass slides for 1 h with 4% paraformaldehyde, washed in PBS and then treated with 0.1% Triton X-100 in PBS. After blocking overnight in PBS/3%BSA, slides were incubated 1 h in primary antibody, washed several times with PBS and then incubated 30 min in fluorescein- or rodamin-conjugated goat α-mouse or α-rabbit secondary antibodies (1:400 dilution). Cell nuclei were labelled with DAPI. The specificity of the immune sera was checked in parallel using pre-immune sera. In double IFA experiments using mouse immune sera against Pbg377 and MDV/PEG3, slides were first incubated with α-Pbg377 immune serum as described above and fixed with 4% paraformaldehyde prior incubation with the second immune serum. α-MDV/PEG3 antibodies were labelled with Zenon kit Alexa Fluor 488 (Invitrogen), according with manufacturer's protocol. Prior labelling IgG were purified from α-MDV/PEG3 immune serum using protein G agarose (Life Technologies). Ten micrograms of labelled IgG were used in IFA.

Western blot analysis

Western blot analysis was performed using MINI TRANS-BLOT® Bio-Rad apparatus at constant voltage (100 V) for 1 h, in transfer buffer (20% methanol, Tris 0,025 M, Glycine 0.192 M) onto Protran 0.22 microns membrane (Whatman). Incubation with antibodies was done. Primary and horseradish peroxidase-conjugated secondary antibody were incubated 1 h in PBS-Tween (0.05%) and membrane was developed using the ECL system (SuperSignalWest Pico, Thermo Scientific) according to manufacturer's instructions.

Acknowledgements

We thank Jai Ramesar for technical support. We thank Leonardo Picci for preparation of the immune serum against Pbg377 used in this study. The research leading to these results has received funding from the European Community's Seventh Framework Programme (FP7/2007–2013) under grant agreement no. 242095 and from the Italian FLAGSHIP 'InterOmics' project (PB.P05) funded by MIUR and coordinated by the CNR. Inga Siden-Kiamos recognizes the support of the OzMalNet fund of the EVIMalaR Network of Excellence for the work carried out at Bio21, University of Melbourne and gratefully acknowledges the support of Ms Vanessa Mollard and Prof. Geoff McFadden. The authors have no conflict of interest.

References

Abkarian, M., Massiera, G., Berry, L., Roques, M., and Braun-Breton, C. (2011) A novel mechanism for egress of malarial parasites from red blood cells. *Blood* **117:** 4118–4124.

Aikawa, M., Carter, R., Ito, Y., and Nijhout, M.M. (1984) New observations on gametogenesis, fertilization, and zygote transformation in *Plasmodium gallinaceum*. *J Protozool* **31:** 403–413.

Alano, P., Read, D., Bruce, M., Aikawa, M., Kaido, T., Tegoshi, T., *et al*. (1995) COS cell expression cloning of Pfg377, a *Plasmodium falciparum* gametocyte antigen associated with osmiophilic bodies. *Mol Biochem Parasitol* **74:** 143–156.

Annoura, T., Ploemen, I.H., van Schaijk, B.C., Sajid, M., Vos, M.W., van Gemert, G.J., *et al*. (2012) Assessing the adequacy of attenuation of genetically modified malaria parasite vaccine candidates. *Vaccine* **30:** 2662–2670.

Billker, O., Lindo, V., Panico, M., Etienne, A.E., Paxton, T., Dell, A., *et al*. (1998) Identification of xanthurenic acid as the putative inducer of malaria development in the mosquito. *Nature* **392:** 289–292.

Billker, O., Dechamps, S., Tewari, R., Wenig, G., Franke-Fayard, B., and Brinkmann, V. (2004) Calcium and a calcium-dependent protein kinase regulate gamete formation and mosquito transmission in a malaria parasite. *Cell* **117:** 503–514.

Blackman, M.J., and Carruthers, V.B. (2013) Recent insights into apicomplexan parasite egress provide new views to a kill. *Curr Opin Microbiol* **16:** 459–464.

Braks, J.A., Mair, G.R., Franke-Fayard, B., Janse, C.J., and Waters, A.P. (2008) A conserved U-rich RNA region implicated in regulation of translation in Plasmodium female gametocytes. *Nucleic Acids Res* **36:** 1176–1186.

Chandramohanadas, R., Park, Y., Lui, L., Li, A., Quinn, D., Liew, K., *et al*. (2011) Biophysics of malarial parasite exit from infected erythrocytes. *PLoS ONE* **6:** e20869.

Deligianni, E., Morgan, R.N., Bertuccini, L., Kooij, T.W., Laforge, A., Nahar, C., *et al*. (2011) Critical role for a stage-specific actin in male exflagellation of the malaria parasite. *Cell Microbiol* **13:** 1714–1730.

Deligianni, E., Morgan, R.N., Bertuccini, L., Wirth, C.C., de Monerri, N.C., Spanos, L., *et al*. (2013) A perforin-like protein mediates disruption of the erythrocyte membrane during egress of *Plasmodium berghei* male gametocytes. *Cell Microbiol* **15:** 1438–1455.

van Dijk, M.R., Janse, C.J., Thompson, J., Waters, A.P., Braks, J.A., Dodemont, H.J., *et al*. (2001) A central role for P48/45 in malaria parasite male gamete fertility. *Cell* **104:** 153–164.

Furuya, T., Mu, J., Hayton, K., Liu, A., Duan, J., Nkrumah, L., *et al*. (2005) Disruption of a *Plasmodium falciparum* gene linked to male sexual development causes early arrest in gametocytogenesis. *Proc Natl Acad Sci USA* **102:** 16813–16818.

Glushakova, S., Yin, D., Li, T., and Zimmerberg, J. (2005) Membrane transformation during malaria parasite release from human red blood cells. *Curr Biol* **15:** 1645–1650.

Hanssen, E., Dekiwadia, C., Riglar, D.T., Rug, M., Lemgruber, L., Cowman, A.F., *et al*. (2013) Electron tomography of *Plasmodium falciparum* merozoites reveals core cellular events that underpin erythrocyte invasion. *Cell Microbiol* **15:** 1457–1472.

Janse, C.J., and Waters, A.P. (1995) *Plasmodium berghei*: the application of cultivation and purification techniques to molecular studies of malaria parasites. *Parasitol Today* **11:** 138–143.

Janse, C.J., Haghparast, A., Speranca, M.A., Ramesar, J., Kroeze, H., del Portillo, H.A., and Waters, A.P. (2003) Malaria parasites lacking eef1a have a normal S/M phase yet grow more slowly due to a longer G1 phase. *Mol Microbiol* **50:** 1539–1551.

Janse, C.J., Ramesar, J., and Waters, A.P. (2006) High-efficiency transfection and drug selection of genetically transformed blood stages of the rodent malaria parasite *Plasmodium berghei*. *Nat Protoc* **1:** 346–356.

de Koning-Ward, T.F., Olivieri, A., Bertuccini, L., Hood, A., Silvestrini, F., Charvalias, K., *et al*. (2008) The role of osmiophilic bodies and Pfg377 expression in female gametocyte emergence and mosquito infectivity in the human malaria parasite *Plasmodium falciparum*. *Mol Microbiol* **67:** 278–290.

Kremer, J.R., Mastronarde, D.N., and McIntosh, J.R. (1996) Computer visualization of three-dimensional image data using IMOD. *J Struct Biol* **116:** 71–76.

Lal, K., Delves, M.J., Bromley, E., Wastling, J.M., Tomley, F.M., and Sinden, R.E. (2009) Plasmodium male development gene-1 (mdv-1) is important for female sexual development and identifies a polarised plasma membrane during zygote development. *Int J Parasitol* **39:** 755–761.

Lanfrancotti, A., Bertuccini, L., Silvestrini, F., and Alano, P. (2007) *Plasmodium falciparum*: mRNA co-expression and protein co-localisation of two gene products upregulated in early gametocytes. *Exp Parasitol* **116:** 497–503.

McRobert, L., Taylor, C.J., Deng, W., Fivelman, Q.L., Cummings, R.M., Polley, S.D., *et al*. (2008) Gametogenesis in malaria parasites is mediated by the cGMP-dependent protein kinase. *PLoS Biol* **6:** e139.

Mastronarde, D.N. (1997) Dual-axis tomography: an approach with alignment methods that preserve resolution. *J Struct Biol* **120:** 343–352.

Mastronarde, D.N. (2005) Automated electron microscope tomography using robust prediction of specimen movements. *J Struct Biol* **152:** 36–51.

Newman, G.R. (1989) LR white embedding medium for

colloidal gold methods. In *Colloidal Gold – Principles, Methods and Applications*, Vol. **2**. Hayat, M.A. (ed.). San Diego: Academic Press, pp. 47–73.

Pace, T., Olivieri, A., Sanchez, M., Albanesi, V., Picci, L., Siden Kiamos, I., *et al*. (2006) Set regulation in asexual and sexual Plasmodium parasites reveals a novel mechanism of stage-specific expression. *Mol Microbiol* **60:** 870–882.

Perry, M.M., and Gilbert, A.B. (1979) Yolk transport in the ovarian follicle of the hen (*Gallus domesticus*): lipoprotein-like particles at the periphery of the oocyte in the rapid growth phase. *J Cell Sci* **39:** 257–272.

Ponzi, M., Siden-Kiamos, I., Bertuccini, L., Curra, C., Kroeze, H., Camarda, G., *et al*. (2009) Egress of *Plasmodium berghei* gametes from their host erythrocyte is mediated by the MDV-1/PEG3 protein. *Cell Microbiol* **11:** 1272–1288.

Pradel, G. (2007) Proteins of the malaria parasite sexual stages: expression, function and potential for transmission blocking strategies. *Parasitology* **134:** 1911–1929.

Saito, N., Konishi, K., Takeda, H., Kato, M., Sugiyama, T., and Asaka, M. (2003) Antigen retrieval trial for post-embedding immunoelectron microscopy by heating with several unmasking solutions. *J Histochem Cytochem* **51:** 989–994.

Severini, C., Silvestrini, F., Sannella, A., Barca, S., Gradoni, L., and Alano, P. (1999) The production of the osmiophilic body protein Pfg377 is associated with stage of maturation and sex in *Plasmodium falciparum* gametocytes. *Mol Biochem Parasitol* **100:** 247–252.

Shupliakov, O., Haucke, V., and Pechstein, A. (2011) How synapsin I may cluster synaptic vesicles. *Semin Cell Dev Biol* **22:** 393–399.

Silvestrini, F., Bozdech, Z., Lanfrancotti, A., Di Giulio, E., Bultrini, E., Picci, L., *et al*. (2005) Genome-wide identification of genes upregulated at the onset of gametocytogenesis in *Plasmodium falciparum*. *Mol Biochem Parasitol* **143:** 100–110.

Sinden, R.E. (1983) Sexual development of malarial parasites. *Adv Parasitol* **22:** 153–216.

Sinden, R.E. (1997) Infection of mosquitoes with rodent malaria. In *Molecular Biology of Insect Disease Vectors: A Methods Manual*. Crampton, J.M., Beard, C.B., and Louis, C. (eds). London.: Chapman and Hall, pp. 67–91.

Sinden, R.E., Canning, E.U., and Spain, B. (1976) Gametogenesis and fertilization in *Plasmodium yoelii nigeriensis*: a transmission electron microscope study. *Proc R Soc Lond B Biol Sci* **193:** 55–76.

Sologub, L., Kuehn, A., Kern, S., Przyborski, J., Schillig, R., and Pradel, G. (2011) Malaria proteases mediate inside-out egress of gametocytes from red blood cells following parasite transmission to the mosquito. *Cell Microbiol* **13:** 897–912.

Spaccapelo, R., Janse, C.J., Caterbi, S., Franke-Fayard, B., Bonilla, J.A., Syphard, L.M., *et al*. (2010) Plasmepsin 4-deficient *Plasmodium berghei* are virulence attenuated and induce protective immunity against experimental malaria. *Am J Pathol* **176:** 205–217.

van Spaendonk, R.M., Ramesar, J., van Wigcheren, A., Eling, W., Beetsma, A.L., van Gemert, G.J., *et al*. (2001) Functional equivalence of structurally distinct ribosomes in the malaria parasite, *Plasmodium berghei*. *J Biol Chem* **276:** 22638–22647.

Talman, A.M., Lacroix, C., Marques, S.R., Blagborough, A.M., Carzaniga, R., Menard, R., and Sinden, R.E. (2011) PbGEST mediates malaria transmission to both mosquito and vertebrate host. *Mol Microbiol* **82:** 462–474.

Wirth, C.C., and Pradel, G. (2012) Molecular mechanisms of host cell egress by malaria parasites. *Int J Med Microbiol* **302:** 172–178.

World Malaria Report (2013). World Health Organization.

Zuccala, E.S., and Baum, J. (2011) Cytoskeletal and membrane remodelling during malaria parasite invasion of the human erythrocyte. *Br J Haematol* **154:** 680–689.

Supporting information

Additional Supporting Information may be found in the online version of this article at the publisher's web-site:

Fig. S1. MOB coalescence is triggered by a drop in temperature. Purified schizonts of the WT line were injected intravenously into a mouse to obtain synchronous blood stages. Tail blood was collected 30 h post-infection to recover mature gametocytes. Infected blood was immediately smeared and fixed in paraformaldehyde (A) or kept 15 min at 22°C and washed in PBS prior fixation (B). Blood smears were then and subjected to IFA.

Fig. S2. Transmission electron micrographs of activated WT gametocytes. (1) TEM images of an activated male (1–2 min after induction) with enlarged nucleus (Nu) and a cluster of MOB in the close vicinity of the plasma membrane (A), 5–8 min after activation axonemes (Ax) are being formed, while the large majority of MOB clusters disappear (B), suggesting that they fuse with parasite plasma membrane and discharge their content into the PV. At difference, OB moves to the periphery of an activated female gametocyte as separate vesicles (C) and discharge their content within 1–2 min (D). (2) IFA of male gametocytes, 5–8 min after induction. Male gamete flagella, stained with antibodies against tubulin-I, are being formed; MDV/PEG3-specific fluorescence is very faint, suggesting that the majority of protein has been discharged. Scale bar: 5 μm.

Fig. S3. Ca^{2+} chelator BAPTA_AM affects OB and MOB localization upon gametocyte activation. Mature gametocytes from a synchronous infection (30 h post-merozoite invasion) were pretreated with the Ca^{2+} chelator BAPTA-AM (100 μM, 20 min at 37°C). The effectiveness of the treatment was monitored by inspecting exflagellations upon gametocyte induction. Exflagellations in treated sample were completely blocked, while normal progression of gametogenesis was observed in the control sample from the same mouse. Blood smears from BAPTA-treated and control parasites were stained with α-Pbg377 (A) or α-MDV/PEG3 (B). In both cases, OB and MOB relocation is hampered.

Fig. S4. Generation and genotyping of mutants lacking Pbg377 (Δ*PbG377*). A. Schematic representation of gene-deletion construct targeting the open reading frame (ORF) of *PbG377* by double crossover homologous recombination, and the wild-type (wt) gene locus before and after disruption in two transfection experiments (exp 600 and 622). The construct contains a drug-selectable marker cassette (SM; white box) and gene target regions (black arrows). See the *Materials and Methods* section for primer sequences used to amplify the target regions.

Restriction sites for diagnostic Southern analysis (see B) are shown. B. Diagnostic Southern analysis of digested genomic DNA (right; BglII) or of pulsed field gel-separated chromosomes (left) confirm correct disruption of *PbG377* in Δ*PbG377* parasites. Separated chromosomes were hybridized with the 3'UTR of *P. berghei dhfr/ts* gene recognizing the endogeneous *dhfr/ts* locus on chromosome 7 and the integrated locus at chromosome 14. Digested DNA (BglII) was hybridized with a probe recognizing the *Tgdhfr/ts* SM (see A for the sizes of the DNA fragments). m: after mosquito passage of Δ*PbG377* parasites. C. Northern analysis confirms the absence *of Pbg377* transcripts in Δ*PbG377* parasites. Northern blots were hybridized with a PCR probe specific for the 5'utr of *PbG377*. As a loading control, blots were hybridized with a Pbs25 specific probe (using a PCR-amplified PBANKA_051500.

Fig. S5. OB morphology and size is affected in *ΔPbG377*. Box-plot of maximum (A) and minimum (B) values of OB size in WT and *ΔPbG377* (128 and 163 sections inspected, respectively). In WT female gametocytes, median of maximum and minimum values is, respectively, 1.7- and 1.5-fold higher than that observed in Δ*PbG377* gametocytes. Data distribution around median show high variance in maximum values of both WT and KO parasites. This is expected for elongated structures and confirm tridimensional reconstruction of OB and MOB.

Fig. S6. Ultrastructural analysis of gametocytes of *ΔPbg377* and *ΔMDV1/PEG3* parasites. A. TEM images of *ΔPbg377* female gametocytes show tiny OB, smaller than OB of *ΔMDV/PEG3* females, which display WT size and morphology. B. In *ΔPbg377* gametocytes, α-MDV/PEG3 stains OB-like structures and normal MOB; in *ΔMDV/PEG3* gametocytes, α-Pbg377 stains OB morphologically similar to OB of the WT parasites.

Fig. S7. OB and MOB behaviour in activated *ΔPbG377* gametocytes. After 1 min of induction, OB stained by MDV/PEG3 antibodies relocate to the gametocyte periphery, while MOB tend to form clusters similar to those observed in WT parasites.

Table S1. Phenotype analyses of Δ*PbG377* parasites during blood and mosquito development.